JOURNAL OF VIROLOGY, Apr. 2010, p. 4060–4072 Vol. 84, No. 8
0022-538X/10/$12.00 doi:10.1128/JVI.01450-09

Impact of Varicella-Zoster Virus on Dendritic Cell Subsets in Human Skin during Natural Infection▽†

Jennifer H. Huch,[1,2] Anthony L. Cunningham,[2] Ann M. Arvin,[3] Najla Nasr,[2] Saskia J. A. M. Santegoets,[4] Eric Slobedman,[5] Barry Slobedman,[2]‡ and Allison Abendroth[1,2]*‡

Discipline of Infectious Diseases and Immunology, University of Sydney, Sydney, New South Wales 2006, Australia[1]; Centre For Virus Research, Westmead Millennium Institute and University of Sydney, Westmead, New South Wales 2145, Australia[2]; Departments of Pediatrics and Microbiology and Immunology, Stanford University School of Medicine, Stanford, California 94305[3]; Department of Pathology, VU University Medical Center, De Boelelaan 1117, Amsterdam 1081HV, Netherlands[4]; and Laverty Pathology, North Ryde, New South Wales, 2113, Australia[5]

Received 14 July 2009/Accepted 8 January 2010

Varicella-zoster virus (VZV) causes varicella and herpes zoster, diseases characterized by distinct cutaneous rashes. Dendritic cells (DC) are essential for inducing antiviral immune responses; however, the contribution of DC subsets to immune control during natural cutaneous VZV infection has not been investigated. Immunostaining showed that compared to normal skin, the proportion of cells expressing DC-SIGN (a dermal DC marker) or DC-LAMP and CD83 (mature DC markers) were not significantly altered in infected skin. In contrast, the frequency of Langerhans cells was significantly decreased in VZV-infected skin, whereas there was an influx of plasmacytoid DC, a potent secretor of type I interferon (IFN). Langerhans cells and plasmacytoid DC in infected skin were closely associated with VZV antigen-positive cells, and some Langerhans cells and plasmacytoid DC were VZV antigen positive. To extend these *in vivo* observations, both plasmacytoid DC (PDC) isolated from human blood and Langerhans cells derived from MUTZ-3 cells were shown to be permissive to VZV infection. In VZV-infected PDC cultures, significant induction of alpha IFN (IFN-α) did not occur, indicating the VZV inhibits the capacity of PDC to induce expression of this host defense cytokine. This study defines changes in the response of DC which occur during cutaneous VZV infection and implicates infection of DC subtypes in VZV pathogenesis.

Varicella-zoster virus (VZV) is a highly species-specific human herpesvirus that causes the diseases varicella (chicken pox) and herpes zoster (shingles). Varicella results from the primary phase of infection and is characterized by a diffuse rash of vesiculopustular lesions that appear in crops and usually resolve within 1 to 2 weeks (7, 26). Primary infection is initiated by inoculation of mucosal sites, such as the upper respiratory tract and the conjunctiva, with infectious virus, usually contained within respiratory droplets (3, 23). Following inoculation, there is a 10- to 21-day incubation period during which VZV is transported to the regional lymph nodes; however, it remains unclear which cell types are responsible for transport of VZV during natural infection (3). It has been hypothesized that dendritic cells (DC) of the respiratory mucosa may be among the first cells to encounter VZV during primary infection and are capable of virus transport to the draining lymph nodes (1, 45). It is postulated that within lymph nodes, VZV undergoes a period of replication, resulting in a primary cell-associated viremia, during which time virus is transported to the reticuloendothelial organs, where it undergoes another period of replication that results in a secondary cell-associated viremia and virus transport to the skin (3, 23). However, VZV has recently been shown to have tropism for human tonsillar $CD4^+$ T lymphocytes (37), and it has been demonstrated that these T lymphocytes express skin homing markers that may allow them to transport VZV directly from the lymph node to the skin during primary viremia (38). Once the virus reaches the skin, it infects cutaneous epithelial cells, resulting in distinctive vesiculopustular lesions.

During the course of primary infection, VZV establishes a lifelong latent infection within the sensory ganglia, from which virus may reactivate years later to cause herpes zoster (22, 42, 53). VZV reactivation results in the production of new infectious virus and a characteristic vesiculopustular rash, which differs from that of varicella insofar as the distribution of the lesions is typically unilateral and covers only 1 to 2 dermatomes (8). In both primary and reactivated VZV infection of human skin, VZV antigens are detectable in the epidermis and dermis (2, 30, 46, 47, 49, 52), and although some studies have examined the immune infiltrate present in these lesions, most have focused on T lymphocytes, macrophages, and NK cells (40, 48, 50, 51, 58). The role of DC subsets in VZV infection in human skin has not been previously explored *in vivo*.

Our laboratory provided the first evidence that VZV could productively infect human immature and mature monocyte-derived dendritic cells (MDDC) *in vitro* (1, 45), and Hu and Cohen (2005) showed that VZV ORF47 was critical for rep-

* Corresponding author. Mailing address: University of Sydney, Discipline of Infectious Diseases and Immunology, Blackburn Building, Room 601, New South Wales 2006, Australia. Phone: 61-2-93516878. Fax: 61-2-93514731. E-mail: a.abendroth@usyd.edu.au.

‡ A.A. and B.S. contributed equally to the manuscript.

† Supplemental material for this article may be found at http://jvi.asm.org/.

▽ Published ahead of print on 3 February 2010.

lication of virus in human immature DC but not mature DC (29). However, whether DC become directly infected during natural VZV skin infection and the impact VZV infection may have on DC subsets has yet to be elucidated. The two subsets of DC that are normally present in the skin and which may be involved in the pathogenesis of VZV infection are the Langerhans cells (LC) of the epidermis and dermal DC (DDC) (60). LC are present in an immature state in uninfected skin and in upper respiratory tract epithelium. Upon capture of foreign antigens, LC have the capacity to migrate from the periphery to the lymph nodes, where they seek interaction with T lymphocytes (60). Although the location of cutaneous DC suggests that they are a DC subset likely to be involved in the pathogenesis of VZV infection, other subsets of DC, such as the blood-derived myeloid DC (MDC) and plasmacytoid DC (PDC), are also potentially important in the pathogenesis of VZV infection. Of particular interest are PDC, since these cells are important in innate antiviral immune responses due to their ability to recruit to sites of inflammation and secrete high levels of alpha interferon (IFN-α) (6, 18, 56). PDC also participate in adaptive immune responses through their secretion of cytokines and chemokines that promote activation of effector cells, including NK cells, NKT cells, B lymphocytes, and T lymphocytes, and also through their capacity to present antigen to T lymphocytes (9, 63). Whether PDC and LC can be infected with VZV and their roles during infection have not been previously studied.

In this study, we sought to identify and compare the subsets of DC present in human skin lesions following natural VZV infection and to assess DC permissiveness to VZV infection. We utilized immunohistochemical (IHC) and immunofluorescent (IFA) staining to characterize DC subsets within the skin of multiple patients with either varicella or herpes zoster, and identified profound changes in the frequency of LC and PDC as a consequence of cutaneous VZV infection. In addition, some LC and PDC costained with a range of VZV antigens indicative of productive infection. PDC isolated from human blood and LC derived from the MUTZ-3 cells were shown to be permissive to productive VZV infection *in vitro*. This study defines changes in the type and distribution of DC during natural cutaneous VZV infection and implicates infection of specific DC subsets in VZV pathogenesis.

MATERIALS AND METHODS

Skin samples and preparation of sections for immunohistochemical and immunofluorescent staining. Samples from varicella skin lesions ($n = 5$), herpes zoster skin lesions ($n = 5$), and uninfected skin ($n = 3$) were each obtained from separate donors by punch biopsy, fixed, and paraffin embedded. The varicella and zoster cases ranged from 3 to 72 h and 72 h to 7 days, respectively, after the first appearance of the rash (Table 1). Samples were obtained with the approval of the University of Sydney and Sydney West Area Health Service Human Research Ethics Committees. Sections were dewaxed, hydrated, and washed for 2 min in Tris-buffered saline (TBS), 50 mM Tris (Amresco), and 150 mM NaCl (Amresco) in distilled water (dH_2O), before blocking of endogenous peroxidase with 3% H_2O_2 (Fronine, Australia) in dH_2O for 5 min. Sections were incubated in unmasking buffer, either 0.01 M citrate buffer (pH 6.0) (AnalaR, Australia) in dH_2O or 1 mM EDTA buffer (pH 8.0) (Gibco) in dH_2O, as determined during antibody optimization, at 95°C for 15 min, after which sections were cooled in unmasking buffer for 20 min at room temperature (RT).

Antibodies. All antibodies used for immunohistochemistry, immunofluorescent staining, and flow cytometry and the dilutions and conditions under which they were used are listed in Table 2.

TABLE 1. Uninfected skin, varicella skin lesion, and herpes zoster skin lesion biopsy specimens used in this study

Case	Condition	Time post-rash onset
U1	Uninfected	NA[a]
U2	Uninfected	NA
U3	Uninfected	NA
V1	Varicella	3 h
V2	Varicella	40 h
V3	Varicella	42 h
V4	Varicella	48 h
V5	Varicella	72 h
HZ1	Herpes zoster	72 h
HZ2	Herpes zoster	72 h
HZ3	Herpes zoster	7 days
HZ4	Herpes zoster	7 days
HZ5	Herpes zoster	7 days

[a] NA, not applicable.

Preparation of cell spots for immunohistochemical and immunofluorescent staining. Cells were centrifuged and resuspended in 10 to 20 μl of phosphate-buffered saline (PBS) (Amresco). The cells were spotted onto Superfrost Plus slides (Menzel-Glaser, Germany), fixed with 4% paraformaldehyde (Electron Microscopy Sciences) for 15 min at RT, and then stored in PBS at 4°C for up to 48 h, until use. Immediately prior to staining, cell spots were permeabilized with 0.2% Triton (Sigma) in PBS for 10 min at RT.

Immunohistochemical staining. Five-micrometer paraffin-embedded sections were washed in TBS for 2 min before blocking serum, either 10% normal goat serum (NGS) (Sigma) in TBS, used with the IDetect super stain system (ID Labs), or 10% normal human serum (NHS) in TBS, used with the Mach4 universal horseradish peroxidase (HRP) polymer kit (Biocare Medical), was applied in a humidified chamber for 30 min at RT. The blocking serum was removed before the primary antibodies were applied in a humidified chamber for 1 h at RT, following which sections were washed for 5 min in TBS. The IDetect super stain system (HRP) was used as specified by the supplier with antibodies against CD1a, langerin, DC-SIGN, CD83, and VZV gE. The Mach4 universal HRP polymer kit was used as recommended by the supplier with antibodies against CD123 and DC-LAMP. The colored enzyme substrate (Vector VIP peroxidase substrate kit; Vector Laboratories) was applied to all sections for 10 min at RT, after which slides were washed for 10 min in TBS. The sections were counterstained with a 1:3 solution of Mayer's hematoxylin (Fronine, Australia) in TBS for 10 s, after which they were washed for 5 min in lukewarm H_2O. Following counterstaining, the slides were dehydrated and allowed to air dry. Ultramount 4 mounting medium (Fronine, Australia) was applied to each section before coverslips (22 by 50 mm; no. 1) (Menzel-Glaser, Germany) were placed on the slides. Slides were then viewed under a light microscope (model DM1000) (Leica Microsystems, Germany).

Dual immunofluorescent staining. Paraffin-embedded sections or cell spots were washed for 2 min in TBS before blocking serum, 20% normal donkey serum (NDS) (Sigma) in TBS, was applied in a humidified chamber for 30 min at RT. The blocking serum was removed before the first primary antibodies were applied in a dark, humidified chamber for 1 h at 37°C, following which sections were washed for 5 min in TBS. Appropriate secondary antibodies were applied to sections in a dark, humidified chamber for 30 min at 37°C, followed by a 5-min wash in TBS. Sections were blocked again, as previously described, with 20% NDS. The blocking buffer was again removed from the slides, following which the second primary antibodies and appropriate secondary antibodies were applied and slides were washed as before. Following the final wash step, 3 to 6 μl of ProLong Gold antifade reagent with 4′,6-diamidino-2-phenylindole (DAPI) (Molecular Probes) was applied to each section or cell spot. Coverslips were mounted, and slides were sealed before viewing under a fluorescence microscope (model BX51) (Olympus).

Human foreskin fibroblast and virus culture. Human foreskin fibroblasts (HFF) were derived from normal human foreskin tissue and used to culture VZV. HFF were grown in tissue culture medium Dulbecco's modified Eagle medium (DMEM) (Gibco) supplemented with 10% heat-inactivated fetal bovine serum (FBS) (CSL, Australia) and penicillin (10,000 U/ml)-streptomycin (10,000 μg/ml) (Gibco) and incubated at 37°C with 5% CO_2. HFF infected with a clinical isolate of VZV, strain Schenke, were used to infect 80%-confluent monolayers of

TABLE 2. Antibodies used in this study

Antibody	Type	Clone	HTU[a] buffer	Dilution[c]	Source
Anti-VZV IE62	Rabbit pAb[b]	NA	Citrate	1:500 (IFp, IFc)	PR Kinchington
Anti-VZV ORF4	Rabbit pAb	NA	Citrate	1:500 (IFp, IFc)	PR Kinchington
Anti-VZV ORF29	Rabbit pAb	NA	Citrate	1:500 (IFp, IFc)	PR Kinchington
Anti-VZV gE	Mouse IgG2b	NA	Citrate	1:10 (IFp), 1:100 (IHC, IFc)	Chemicon International
Anti-human CD1a	Mouse IgG1	MTB1	Citrate	1:10 (IHC)	NovoCastra
Anti-human langerin	Mouse IgG2b	12D6	Citrate	1:100 (IHC, IFp)	NovoCastra
Anti-human CD83	Mouse IgG2b	HB15a	Citrate	1:10 (IHC)	Immunotech
Anti-human DC-LAMP	Mouse IgG1	104.G4	Citrate	1:5 (pdIHC)	Immunotech
Anti-human DC-SIGN–PE	Mouse IgG2b	120507	Citrate	1:500 (IHC)	R&D Systems
Anti-human CD123	Mouse IgG1	9F5	EDTA	1:10 (pdIHC)	BD Biosciences
Anti-human DLEC (BDCA-2)	Goat pAb IgG	NA	Citrate	1:10 (IFp), 1:50 (IFc)	R&D Systems
Anti-human CD83-FITC	Mouse IgG1	HB15e	NA	1:20 (FC)	BD Biosciences
Anti-human DC-SIGN–FITC	Mouse IgG2b	DCN46	NA	1:20 (FC)	BD Biosciences
Anti-human Lin-1–FITC	Mouse MAb mix	NA	NA	1:20 (FC)	BD Biosciences
Anti-human CD123-PE	Mouse IgG1	9F5	NA	1:20 (FC)	BD Biosciences
Anti-human langerin-PE	Mouse IgG1	DCGM4	NA	1:20 (FC)	Coulter Immunotech
Anti-human HLA-DR–PerCP	Mouse IgG2a	L243	NA	1:20 (FC)	BD Biosciences
Anti-human CD11c-APC	Mouse IgG2b	S-HCL-3	NA	1:20 (FC)	BD Biosciences
Anti-human CD123-APC	Mouse IgG2a	AC145	NA	1:20 (FC)	Miltenyi Biotec
Anti-human MR-APC	Mouse IgG1	19.2	NA	1:20 (FC)	BD Biosciences
Anti-human CD1a-PE-Cy5	Mouse IgG1	HI149	NA	1:20 (FC)	BD Biosciences
Mouse IgG1 isotype control	Mouse IgG1	NA	NA	NA	BD Pharmingen
Mouse IgG2a isotype control	Mouse IgG2a	NA	NA	NA	BD Pharmingen
Mouse IgG2b isotype control	Mouse IgG2b	NA	NA	NA	BD Pharmingen
Whole rabbit serum	NA	NA	NA	NA	Sigma
Goat IgG isotype control	Goat pAb	NA	NA	NA	R&D Systems

[a] HTU, high-temperature unmasking.
[b] pAb, polyclonal antibody.
[c] IFp, immunofluorescent staining on paraffin sections; IFc, immunofluorescent staining on cell spots; IHC, immunohistochemistry; pdIHC, immunohistochemistry with polymer detection; FC, flow cytometry.

uninfected HFF to propagate the virus. At 2+ to 3+ cytopathic effect (CPE), where 1+ represented 10% and 4+ represented 100% of the cell monolayer showing plaque formation, VZV-infected monolayers were harvested. To harvest both uninfected and VZV-infected HFF, medium was removed from the flask and cells were washed with PBS at RT. Following aspiration of the PBS, cells were dislodged following incubation with trypsin-EDTA (Invitrogen) for 5 min at 37°C. Following trypsinization, cells were resuspended in 5 ml of PBS and counted using a hemocytometer.

Isolation of PBMC and PDC. Peripheral blood mononuclear cells (PBMC) were separated from buffy coats (Australian Red Cross Blood Bank, Australia) by density gradient sedimentation on Ficoll-Paque medium (GE Healthcare, United Kingdom). T lymphocytes and monocytes within the PBMC population were depleted by incubating PBMC with anti-CD3 and anti-CD14 microbeads (Miltenyi, Germany) and then running the PBMC through two CS columns (Miltenyi, Germany) in a magnetic field. Plasmacytoid DC (PDC) were then positively selected by incubating the remaining PBMC with FcR blocking reagent (Miltenyi, Germany) and anti-CD304 microbeads (Miltenyi, Germany) and running the cells through an MS column (Miltenyi, Germany) in a magnetic field. The bound cells were removed by plunging 1 ml of MACSwash (1% AB serum [Sigma]–5 mM EDTA [Gibco] in PBS) through the column. This positively selected cell fraction was then run through a second MS column to increase the purity of the isolated PDC population. Approximately 3×10^4 PDC were then analyzed by flow cytometry to determine the purity of the isolated PDC population. The isolated PDC sample was stained with anti-Lin-1—fluorescein isothiocyanate (FITC), anti-CD123-phycoerythrin (PE), anti-HLA-DR—peridinin chlorophyll protein (PerCP), and anti-CD11c-allophycocyanin (APC) (Table 2) as described and analyzed on a FACSAria flow cytometer (BD Biosciences). PDC were defined as cells staining positive for CD123 and HLA-DR and staining negative for Lin-1 and CD11c. PDC were maintained in culture in RPMI 1640 supplemented with 10% human AB serum and 5 ng/ml interleukin 3 (IL-3) (R&D Systems).

Infection of PDC. PDC were cultured with uninfected HFF or VZV-infected HFF at a ratio of 2 HFF:1 PDC in a volume of medium that resulted in a total cell concentration of 1,000 cells/μl. Uninfected HFF and VZV-infected HFF were cultured separately as controls in a volume of medium that resulted in a cell concentration of 1,000 cells/μl. Cultures were then incubated for 24 h at 37°C in an atmosphere of 5% CO_2 in air. In some experiments, the Toll-like receptor (TLR) agonist ODN2216 (InvivoGen) was added at a concentration of 2.5 μM.

Generation of LC from MUTZ-3 cells. MUTZ-3 is a human $CD34^+$ acute myeloid leukemia cell line provided by S. Santegoets (VU University Medical Center, Netherlands). MUTZ-3 cells can be induced to acquire an LC-like phenotype and have been used in the study of other virus-LC interactions (12, 39, 43, 55). MUTZ-3 cells were initially cultured at a concentration of 0.1×10^6 cells/ml in minimal essential medium (MEM)-alpha containing ribonucleosides and deoxyribonucleosides (Invitrogen, Australia) and supplemented with 10% conditioned medium from the human renal carcinoma cell line 5637, 20% heat-inactivated FBS (CSL, Australia), penicillin (10,000 U/ml)-streptomycin (10,000 μg/ml) (Gibco), and 50 μM β-mercaptoethanol (Sigma) in a 12-well tissue culture plate with each well containing 2 ml of medium. After 7 days in culture at 37°C with 5% CO_2, the MUTZ-3 cells were collected and resuspended in MEM-alpha as described above, additionally supplemented with 100 ng/ml granulocyte-macrophage colony-stimulating factor (GM-CSF) (Invitrogen, Australia), 2.5 ng/ml tumor necrosis factor alpha (TNF-α) (R&D Systems), and 5 ng/ml transforming growth factor β1 (TGF-β1) (R&D Systems) at a concentration of 0.25×10^6 cells/ml in a 12-well tissue culture plate with each well containing 2 ml of medium to differentiate the MUTZ-3 cells into LC. After 3 days in culture at 37°C with 5% CO_2, medium and cytokines were replenished as per 1 ml per well, and this was again repeated on day 7. On day 10 post-cytokine stimulation, cells were harvested. Approximately 1×10^5 MUTZ-3-derived cells were then analyzed by flow cytometry to confirm the phenotype of the MUTZ-3-derived cells as being LC-like. The MUTZ-3-derived LC sample was stained with anti-langerin-PE (CD207), anti-DC-SIGN-FITC (CD209), anti-mannose receptor (MR)-APC (CD206), anti-CD1a-PE-Cy5, and anti-CD83-FITC as described above and analyzed on a FACSCanto flow cytometer (BD Biosciences) and with FlowJo fluorescence-activated cell sorter (FACS) analysis software (BD Biosciences). Immature MUTZ-3-derived LC were defined as cells staining positive for langerin and CD1a and negative for DC-SIGN, mannose receptor, and CD83-like authentic immature epithelial LCs *in situ*.

Culture of human renal carcinoma cell line 5637. Human renal carcinoma cell line 5637 (Deutsche Sammlung von Mikroorganismen und Zellkulturen GmbH [DSMZ], Germany) was seeded at a concentration of 0.5×10^6 cells/ml in 30 ml of tissue culture medium RPMI (Gibco) supplemented with 10% heat-inacti-

vated FBS (CSL, Australia) in a 180-cm^2 tissue culture flask and incubated at 37°C with 5% CO_2. The cells were allowed to become confluent, following which the medium was aspirated and replaced with fresh medium. The cells were cultured for up to a further 48 h, after which the medium was collected to be used as conditioned medium. To prepare the conditioned medium, the medium was centrifuged at 1,500 rpm for 10 min, filtered through a 0.2-μm filter to remove cell debris, and then stored at −80°C until use.

Infection of MUTZ-3-derived LC. In a tissue culture plate, MUTZ-3-derived LC were cultured in separate wells containing uninfected HFF or VZV-infected HFF at a ratio of 2 HFF:1 LC in a volume of medium that resulted in a total cell concentration of 500 cells/μl. The medium in which the HFF and LC cultures were incubated was supplemented with GM-CSF, TNF-α, and TGF-β1 as described previously for the generation of LC from MUTZ-3 cells. Cultures were then incubated for 3 days at 37°C in an atmosphere of 5% CO_2 in air, and at the end of the culture period the cells were harvested to make cell spots, as described earlier.

Immunostaining and flow cytometry. Cells (5×10^5) were washed once by adding 1 ml of FACS buffer (1% fetal calf serum [FCS], 10 mM EDTA in PBS) (Gibco) to each tube, centrifuging at 1,500 rpm for 5 min, and then aspirating dry. Cells were incubated with appropriate fluorochrome-conjugated antibodies and diluted in FACS buffer in the dark at 4°C for 20 min, following which they were washed once more. Cells were fixed with 1% paraforaldehyde (Electron Microscopy Sciences) in PBS prior to analysis on a FACSAria flow cytometer (BD Biosciences).

Cell counting methods. Quantitative evaluation of numbers of cells stained positive by immunohistochemistry for the various immune cell markers on uninfected, varicella, and herpes zoster skin sections was performed by analyzing 10 ×40-magnified fields of epidermis and 30 ×40 fields of dermis, measuring 10 fields across and 3 fields deep, with a graticule. The graticule grid covered 0.13 mm^2 of tissue, which was identified as epidermis or dermis based on histology. After obtaining a total count of the number of positive cells in each region of tissue for each marker, for each case, the frequency of cells stained positive for each marker per square millimeter of tissue was obtained. Quantitative evaluation of numbers of cells stained positive for the BDCA-2, langerin, and VZV proteins by immunofluorescence on normal, varicella, and herpes zoster skin sections was performed by photographing 10 ×40 fields of epidermis and 10 ×40 fields of dermis. Single-color photos were first taken through each filter and were then merged. After obtaining a total count of the number of BDCA-2^+ or langerin$^+$ cells and VZV$^+$ cells in each region of tissue for each marker combination for each case, the frequency per square millimeter of tissue was calculated. Quantitative evaluation of numbers of cells stained positive for the langerin and VZV proteins and the BDCA-2 and VZV proteins by immunofluorescence on MUTZ-3-derived LC and PDC cell spots, respectively, was performed by photographing 25 magnification-×40 fields in a five-field by five-field square. Single-color photos were first taken through each filter and were then merged. After a total count of the number of total cells, BDCA-2^+ cells, VZV$^+$ cells, and dually positive cells was obtained, the number of dually positive cells was expressed as a percentage of BDCA-2^+ cells. A similar approach was used to elucidate the percentage of langerin$^+$ cells expressing VZV antigens.

ELISA. Supernatant from cultures of PDC cultured with ODN2216, uninfected HFF, or VZV-infected HFF was analyzed for the presence of IFN-α using a human IFN-α serum sample enzyme-linked immunosorbent assay (ELISA) kit (PBL Biomedical Laboratories), as per the directions of the manufacturer.

RESULTS

Frequency and distribution of DC subsets during natural cutaneous VZV infection. To determine the nature and distribution of different DC subsets during natural cutaneous VZV infection, sections of punch biopsy specimens from varicella and herpes zoster skin lesions and from uninfected skin were immunohistochemically stained with a panel of DC markers: CD1a and langerin (LC), DC-SIGN (dermal DC [DDC]), CD83 and DC-LAMP (mature DC), and CD123 and BDCA-2 (PDC). Each sample of VZV-infected skin tested was also stained with the appropriate isotype control antibodies. Multiple 5-μm sections from skin biopsy specimens from five separate varicella, five separate herpes zoster, and three uninfected (normal) cases were examined, and the frequency of antigen-positive cells per mm^2 in both the epidermis and dermis was calculated (Fig. 1; see also Fig. S1 in the supplemental material). Cells expressing CD1a or langerin were readily detected in the epidermis of uninfected skin but rarely detected in the dermis. This observation is consistent with the typical distribution of resident LC in normal skin (60). In stark contrast, the number of cells expressing CD1a or langerin dropped dramatically in the epidermis of VZV-infected skin from both varicella and herpes zoster cases. This decrease was not due to a general loss of cells within the epidermis, since counts of total cells within the epidermis remained comparable between uninfected and VZV-infected skin samples (data not shown). However, the decrease in frequencies of CD1a and langerin-positive cells were observed to be greatest immediately surrounding the lesion, with staining for CD1a and langerin in the histologically normal skin distant from the lesion being comparable to that of uninfected skin.

Cells expressing a DDC marker, DC-SIGN, were not present in the epidermis in uninfected specimens, nor did they appear in the epidermis of either varicella or herpes zoster biopsy specimens. DC-SIGN-expressing cells were detected at a low level in the dermis of normal, varicella, and herpes zoster cases, and the frequencies of detection were comparable between these samples. Similarly, cells expressing a mature DC marker (DC-LAMP) or CD83 were either absent or present at very low levels in the epidermis and dermis of normal skin. With the exception of a small increase in the number of cells expressing CD83 in the epidermis of herpes zoster cases, the frequency of cells expressing these markers did not appear to change as a consequence of cutaneous VZV infection. There was a striking influx of cells expressing the PDC-specific marker (BDCA-2) in the dermis of VZV-infected skin from both varicella and herpes zoster cases in comparison to findings for uninfected skin. This influx was observed to a lesser degree in the epidermis. In addition, there was an increase in the number of cells expressing CD123, which is also expressed by PDC, in the dermis of VZV-infected skin from both varicella and herpes zoster cases in comparison to uninfected skin.

These analyses reveal changes in the distribution of cells expressing different DC subset markers in response to cutaneous VZV infection. In particular, cells expressing markers of LC decreased dramatically in the epidermis in both varicella and herpes zoster, whereas cells expressing the PDC marker BDCA-2 increased in frequency in the dermis and epidermis in both varicella and herpes zoster.

In addition to assessing DC subsets, sections were also examined by IHC for the presence of VZV glycoprotein E (gE). Normal skin incubated with anti-gE antibody yielded no specific staining and showed a normal histological profile, indicated by a well-defined epidermis and dermis (Fig. 2C). Sections from varicella and herpes zoster skin lesions contained vesicles which were located predominantly within the epidermis and which contained large numbers of VZV gE-positive cells (Fig. 2A and data not shown). Notably, gE was detected not only in and around the lesion but also within distinct regions of infiltrating cells deeper within the dermis (Fig. 2A). Consecutive sections of VZV-infected skin stained with isotype control antibody showed no positive staining (Fig. 2B). Taken together, these analyses revealed that VZV infection, which occurred in regions of the epidermis and deeper within the

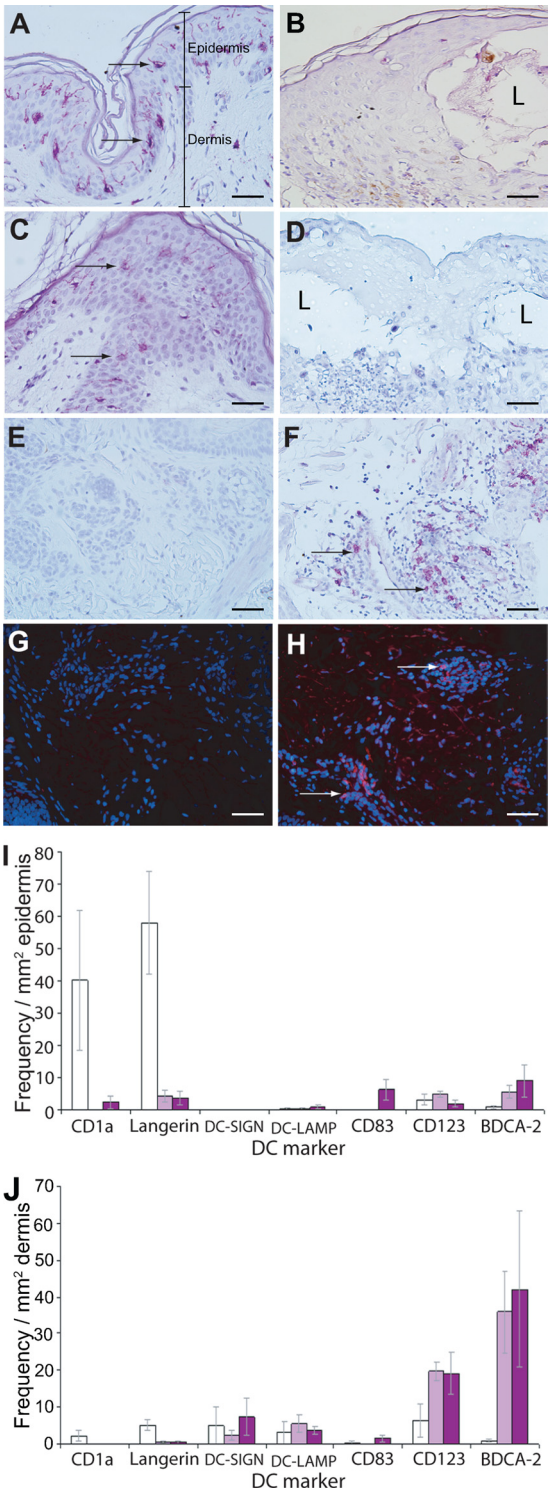

FIG. 1. Frequency and distribution of DC subsets in VZV-infected skin. Immunohistochemical staining (purple) of sections of uninfected skin (A, C, and E) and VZV-infected skin (B, D, and F) for the Langerhans cell markers CD1a (A and B) and langerin (C and D) and for the plasmacytoid DC marker CD123 (E and F). Sections were lightly counterstained by hematoxylin. Immunofluorescent staining (red) for the plasmacytoid DC (PDC) marker BDCA-2 on uninfected skin (G) and VZV-infected skin (H) is shown. Sections were stained with DAPI to reveal cell nuclei (blue). Examples of positively stained cells are indicated by arrows, with BDCA-2-positive PDC shown in panels F and H being deeper within the dermis. Images were captured under magnification ×40, with scale bars representing 50 μm. I and J plot the mean frequency (± SEM) of cells stained positive for a variety of DC markers in the epidermis and dermis, respectively, of uninfected skin (3 donors; white bars), varicella skin (5 donors; light purple bars), and herpes zoster lesions (5 donors; dark purple bars).

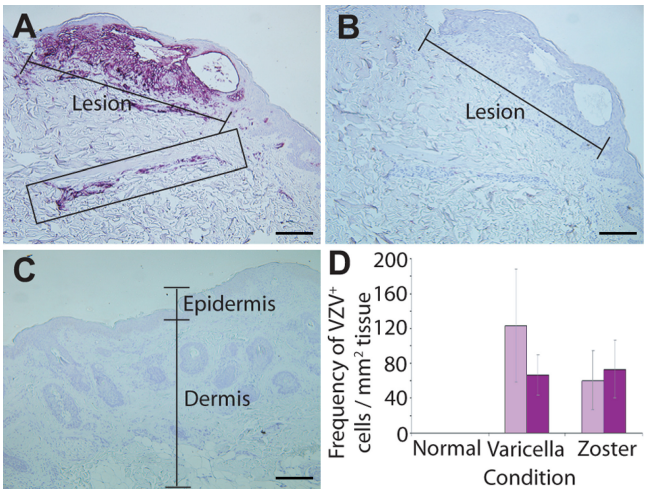

FIG. 2. Distribution of VZV antigen during natural cutaneous VZV infection. Immunohistochemical staining (purple) for VZV glycoprotein E (gE) in skin biopsy specimens of a varicella lesion (A) or uninfected skin (C) is shown. Infiltrating cells staining positive for VZV gE in the dermis of skin from the varicella skin biopsy specimen are boxed. A consecutive section from the varicella skin biopsy specimen stained with an isotype control antibody is shown in panel B. Images were captured under magnification ×10, with scale bars representing 200 μm. (D) Mean frequency (± SEM) of VZV gE-positive cells in skin from uninfected (3 donors), varicella (5 donors), and herpes zoster (5 donors) samples within the epidermis (light purple bars) or dermis (dark purple bars) is plotted.

dermis, was accompanied by changes in the frequency of distinct DC subsets within these regions.

Relationship between VZV antigen-positive cells and dendritic cell subsets in naturally infected skin. To more closely examine the distribution of PDC and LC in the context of cells infected with VZV, the immunostaining approach was modified to encompass a dual immunofluorescence assay (IFA) such that the presence of both DC and VZV antigens could be examined in the same skin biopsy section. Thus, sections were stained for the PDC marker BDCA-2 in combination with antibody against a VZV regulatory protein encoded by ORF4 or the LC marker langerin in combination with VZV ORF4 (Fig. 3). Each sample of VZV-infected skin tested was also stained with the appropriate isotype control antibodies in addition to normal skin being stained with the anti-ORF4 and DC-specific antibodies.

In VZV-infected skin from both varicella and herpes zoster cases subjected to IFA, the distribution of each DC type was comparable to that observed by IHC staining. That is, langerin$^+$ LC were rarely detected in the epidermis, whereas there was a striking influx of BDCA-2$^+$ PDC in the dermis. In contrast, in normal skin, langerin$^+$ LC were readily detected in the

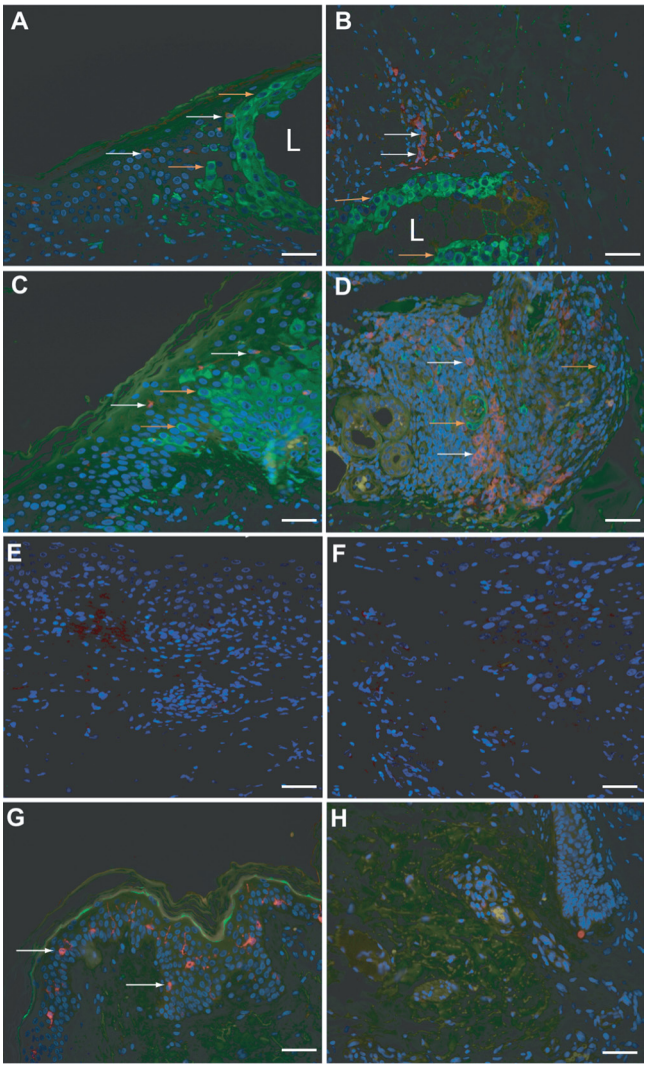

FIG. 3. Detection of VZV antigens and DC subsets in skin during natural cutaneous VZV infection. Dually immunofluorescently stained sections of varicella skin lesion (A and B, cases V2 and V1, respectively) and herpes zoster skin lesion (C and D, cases HZ2 and HZ1, respectively) for combinations of DC markers and VZV antigen are shown. Panels A and C show staining for the Langerhans cell marker langerin (red) in combination with staining for VZV (green) in the epidermis. Panels B and D show staining for the plasmacytoid DC marker BDCA-2 (red) in combination with staining for the VZV (green) in the dermis, with panel B showing an area closer to the lesion and panel D showing an area deeper within the dermis. Panels E and F show isotype control stained sections from varicella and herpes zoster skin samples, respectively. Panels G and H show staining of uninfected skin for langerin and VZV in the epidermis (G) and for BDCA-2 and VZV in the dermis (H). All sections were stained with DAPI to mark cell nuclei (blue). Images were captured under magnification ×40, with scale bars representing 50 μm. Examples of langerin and BDCA-2-positive cells are indicated by white arrows, and examples of VZV-positive cells are indicated by orange arrows. The location of a VZV lesion (L) is indicated when it was present within the field of view.

epidermis and BDCA-2+ PDC were not observed in the dermis. VZV antigens were readily detected in the epidermis surrounding the lesion and also deeper in the dermis in close proximity to regions of infiltrating cells which included the largest concentration of PDC (Fig. 3). No VZV staining was observed in the normal control skin sections.

In some cases, cells were observed that were dually positive for BDCA-2 and VZV antigen or langerin and VZV antigen. These were observed sporadically in both varicella and herpes zoster sections (see Fig. S2 in the supplemental material). To determine whether these VZV antigen-positive DC represented bone fide infected DC, dual immunofluorescent staining was performed for either BDCA-2 or langerin in conjunction with a range of VZV antigens representing different kinetic classes of genes expressed during the productive virus replication cycle. The full replicative cycle of VZV in permissive cells follows a regulated cascade of gene expression. These viral genes can be divided into 3 temporal classes, immediate-early (IE), early (E), and late (L) gene products, based upon their expression kinetics (24). The VZV proteins IE62 and ORF4 are IE proteins that are among the first proteins to be translated during productive VZV infection. Next to be translated is the E class of proteins, of which ORF29 is a member. VZV gE is one of the glycoproteins embedded in the viral envelope, and as a member of the L gene kinetic class, it is among the final viral proteins to be produced during productive VZV infection. Thus, sections were stained by IFA for (i) BDCA-2 in combination with VZV IE62, ORF4, or glycoprotein E (gE) and (ii) langerin in combination with VZV IE62, ORF4, or ORF29 (Fig. 4).

Dually positive cells were not observed for every case examined; however, for some cases, LC or PDC that had stained positive for more than one VZV protein were present. In cases of both varicella and herpes zoster, gE-positive staining was most often observed in PDC, which if observed alone may suggest that these PDC have acquired VZV antigen by uptake of an infected cell and have not actually been productively infected themselves. However, in cases of both varicella and herpes zoster, LC and PDC were detected and stained positive for IE62, ORF4, and ORF29, with the localization of the VZV proteins being indicative of productive infection (31, 32). Neither VZV-infected nor normal control skin stained positive when isotype control antibodies for VZV antigens and DC markers were used. The specificity of VZV antigen detection was further confirmed by a lack of staining when each VZV-specific antibody was used on normal skin sections (Fig. 4). These results suggest that both LC and PDC become productively infected with VZV during the course of natural cutaneous VZV infection.

Permissiveness of plasmacytoid DC and MUTZ-3-derived LC to VZV infection *in vitro*. Given our detection of VZV antigen-positive PDC and LC in human skin during natural VZV infection, we sought to determine whether PDC and LC were permissive to VZV infection *in vitro*. PDC were isolated from fresh peripheral blood mononuclear cells (PBMC) from healthy donors by magnetic bead separation by first depleting $CD3^+$ and $CD14^+$ cells, followed by positive selection for $CD304^+$ cells, and their phenotype was determined by flow cytometry to confirm that they were $CD123^+$ HLA^- DR^+ Lin-1^- $CD11c^-$ PDC. LC were derived from the human acute myeloid leukemia cell line MUTZ-3 using GM-CSF, TNF-α, and TGF-β1, following which their phenotype was confirmed by flow cytometry as being positive for the LC markers langerin and CD1a and negative for DC-SIGN, mannose receptor, and

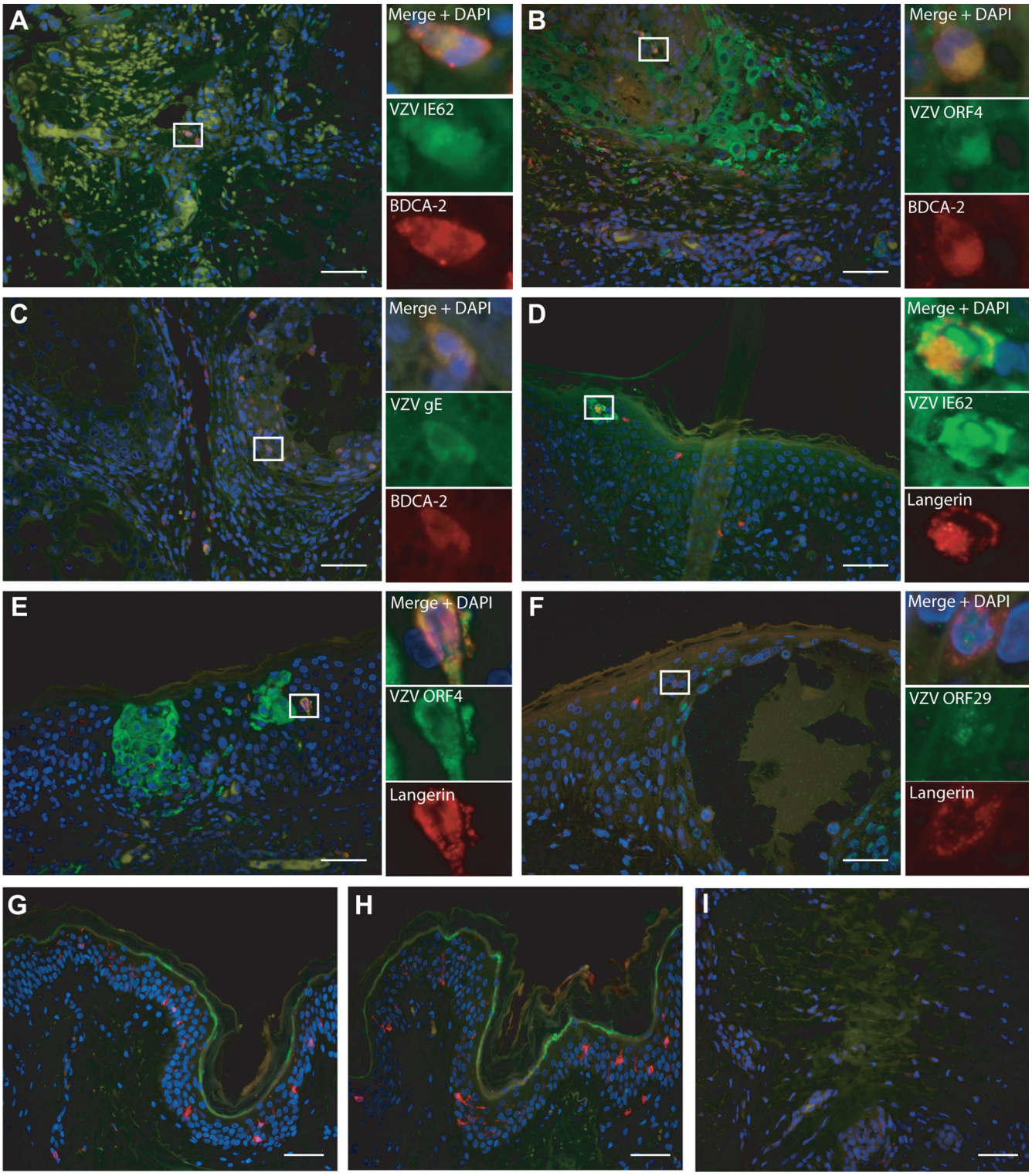

FIG. 4. VZV antigens detected in LC and PDC during natural cutaneous VZV infection. Sections of varicella and herpes zoster skin lesions were dually immunofluorescently stained for combinations of DC markers and VZV antigens, showing the presence of dually positive cells. (A to C) Sections stained for the plasmacytoid DC marker BDCA-2 (red) in combination with staining for VZV antigens IE62 (A) (case HZ1), ORF4 (B) (case HZ3), or gE (C) (case HZ3) (green). (D to F) Sections stained for the Langerhans cell marker langerin (red) in combination with staining for VZV antigens IE62 (D) (case V2), ORF4 (E) (case V2), or ORF29 (F) (case V2) (green) are shown. (G to I) Staining of uninfected skin for langerin and IE62 (G), langerin and ORF29 (H), or BDCA-2 and gE (I) is shown. All sections were stained with DAPI to mark cell nuclei (blue). The main images were captured under magnification ×40, with scale bars representing 50 μm. Examples of dually positive cells are boxed and shown at higher magnification as insets for each staining combination.

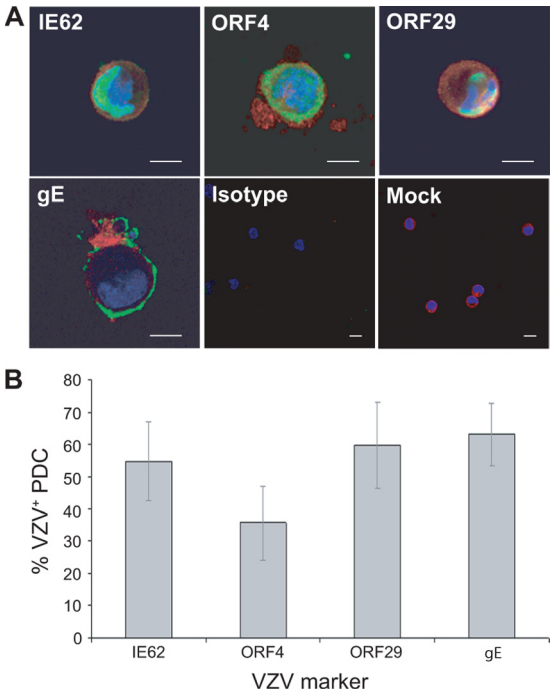

FIG. 5. PDC *in vitro* are permissive to VZV infection. (A) Dual immunofluorescent staining of plasmacytoid DC exposed to VZV for the plasmacytoid DC marker BDCA-2 (red) and VZV antigen IE62, ORF4, ORF29, or gE (green). Staining with isotype control antibodies and mock-infected plasmacytoid DC stained for BDCA-2 and VZV IE62 are also shown. Scale bars, 20 μm. (B) The percentage (± SEM) of BDCA-2$^+$ cells costaining for each VZV antigen from 4 independent replicate experiments.

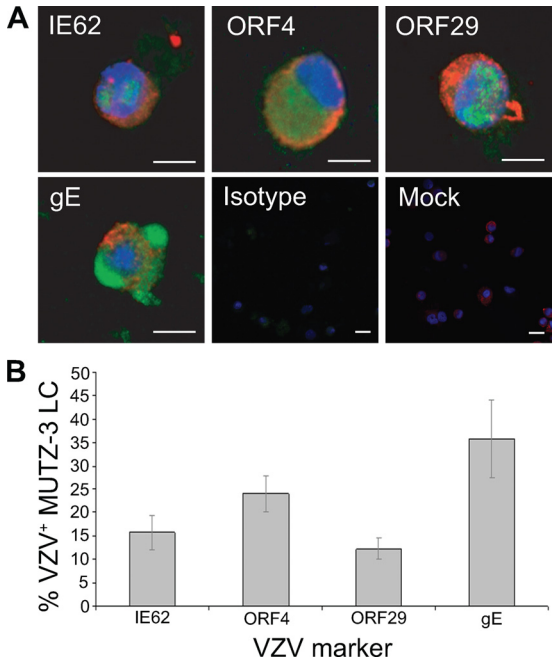

FIG. 6. MUTZ-3-derived LC are permissive to VZV infection. (A) Dual immunofluorescent staining of MUTZ-3-derived LC exposed to VZV for the LC marker langerin (red) and VZV antigen IE62, ORF4, ORF29, or gE (green). Staining with isotype control antibodies and mock-infected MUTZ-3 LC stained for langerin and VZV IE62 are also shown. Scale bars, 20 μm. (B) The percentage (± SEM) of langerin$^+$ cells costaining for each VZV antigen from 3 independent replicate experiments.

CD83. We assessed the susceptibility of these PDC and MUTZ-3-derived LC to VZV infection. VZV is highly cell associated in cell culture, and high-titer cell-free stocks cannot be generated (5, 21, 25, 61, 62). Thus, we infected PDC and MUTZ-3-derived LC with cell-associated VZV by culturing the cells in the presence of VZV-infected human foreskin fibroblasts (HFF) or uninfected HFF. We have previously used this method of infection to demonstrate productive infection of monocyte-derived DC (1, 45). After 24 h, the cells were collected and were used to make cell spots, which were then costained by IFA for the VZV markers IE62, ORF4, ORF29 and gE in combination with BDCA-2 for the PDC (Fig. 5) and langerin for the MUTZ-3-derived LC (Fig. 6).

VZV antigens were readily detected in both BDCA-2$^+$ PDC and langerin$^+$ MUTZ-3-derived LC inoculated with VZV-infected HFF. Representative images of dually positive cells were captured by confocal microscopy (Fig. 5A and 6A). The immediate-early VZV proteins IE62 and ORF4 localized to the nuclei and cytoplasms, respectively, of BDCA-2$^+$ PDC and langerin$^+$ MUTZ-3-derived LC. The early gene product ORF29 showed nuclear localization, and the late viral antigen gE localized to the cytoplasm and cell surface of BDCA-2$^+$ PDC and langerin$^+$ MUTZ-3-derived LC. The subcellular localization of the viral gene products we observed in PDC and langerin$^+$ MUTZ-3-derived LC was consistent with that previously reported for productive infection of permissive cells, such as human fibroblasts and human immature and mature MDDC (1, 45). Although not a direct measure of infectious virus production, the detection of viral antigens from all three kinetic classes is indicative of replicating virus, with this approach having been used previously to define replicating VZV in other cell types infected with cell-associated virus (1, 28, 45). Neither VZV-infected nor mock-infected PDC nor langerin$^+$ MUTZ-3-derived LC populations stained positive when isotype control antibodies for BDCA-2 or langerin and VZV antigens were used in parallel. The proportion of BDCA-2$^+$ PDC expressing viral antigens was determined from four independent experiments using four different blood donors, and the proportion of langerin$^+$ MUTZ-3-derived LC expressing viral antigens was determined from three independent experiments (Fig. 5B and 6B). This analysis demonstrated that a significant proportion of both PDC and MUTZ-3-derived LC became viral antigen positive and that viral antigens from all three kinetic classes were represented in these cells. Furthermore, there was no significant difference between the percentages of cells positive for any of the four VZV antigens detected in PDC or MUTZ-3-derived LC. It was concluded that human PDC and MUTZ-3-derived LC are permissive to VZV infection and are likely to support the full virus replicative cycle.

IFN-α production by PDC cultured with VZV-infected HFF. The most distinctive functional characteristic of PDC is their ability to synthesize IFN-α (6, 9, 18, 56, 63). Thus, we assessed the impact of VZV infection of PDC on IFN-α synthesis. PDC were cultured for 24 h with mock-infected or VZV-infected HFF before supernatants were collected and the amount of

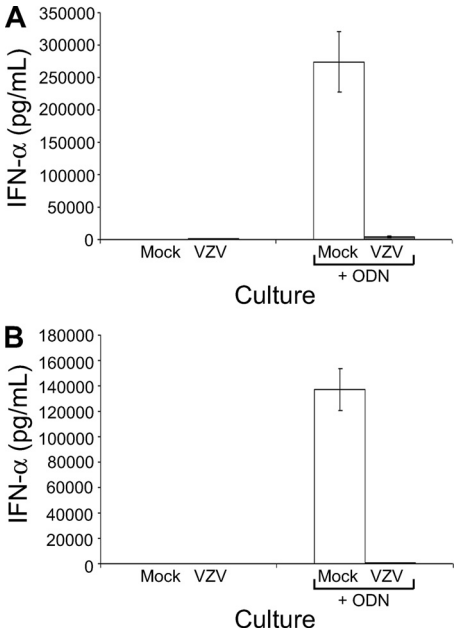

FIG. 7. VZV infection of PDC *in vitro* impacts IFN-α synthesis. Measurement by ELISA of IFN-α secreted from plasmacytoid DC cultures of either mock-infected PDC (white bars) or VZV-infected PDC (gray bars) infected for 24 h or infected for 12 h and then treated with a 2.5 μM concentration of the TLR agonist ODN2216 (ODN) to induce IFN-α production is shown. Panels A and B show results from 2 independent replicate experiments. Error bars show the range of values from duplicate samples for each replicate.

IFN-α measured by ELISA. In two independent replicate experiments, cultures of PDC infected with VZV showed little or no change in the amount of secreted IFN-α, which remained at levels comparable to those of mock-infected PDC cultures (Fig. 7). Assessment of PDC cultures at 8, 12, and 36 h postinfection did not yield any higher levels of IFN-α secretion (data not shown). As a positive control for capacity to induce IFN-α, mock-infected PDC were also cultured for 24 h with 2.5 μM ODN2216, a TLR9 agonist which stimulates IFN-α production by PDC (36). This treatment induced high levels of secreted IFN-α by mock-infected PDC cultures. In contrast, VZV-infected PDC cultures yielded little IFN-α when treated with ODN2216 (Fig. 7).

In addition to assessing IFN-α production by PDC, culture supernatants from VZV-infected HFF (which were used for inoculating PDC) were assessed for IFN-α production by ELISA. In nine independent replicate experiments examining VZV-infected HFF, six experiments showed no detectable IFN-α production and three experiments showed extremely low levels (10 to 30 pg/ml) (data not shown). Thus, VZV-infected HFF produce negligible levels of IFN-α. At 24 h postinfection, there was no significant difference in PDC viability between mock and infected cultures as determined by flow cytometric analysis of propidium iodide (PI) and annexin V staining on gated PDC (data not shown). Taken together, these results demonstrate that VZV is capable of infecting PDC but that infection does not induce significant IFN-α production and infected PDC cultures remain refractory to IFN-α induction even when stimulated with ODN2216.

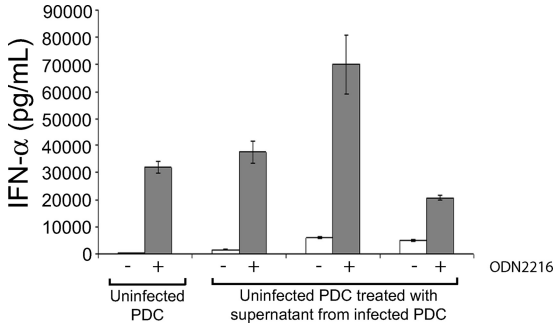

FIG. 8. IFN-α synthesis by uninfected PDC exposed to supernatant from VZV-infected PDC cultures. Measurement by ELISA of IFN-α secreted from uninfected PDC or from uninfected PDC treated with supernatant from VZV-infected PDC after treatment with (gray bars) or without (white bars) 2.5 μM ODN2216 is shown. Treatment of uninfected PDC with supernatant from three independent VZV-infected PDC cultures is shown. The graph shows the level of IFN-α produced by each culture (in pg/ml) along the *y* axis against each culture condition along the *x* axis.

To determine whether a factor secreted from infected PDC renders uninfected bystander PDC defective in their capacity to secrete IFN-α, we removed culture supernatants from VZV-infected PDC cultures and incubated these supernatants with uninfected PDC cultures for 24 h before measuring secreted IFN-α by ELISA. Analysis of three independent replicates revealed only very low levels of IFN-α, demonstrating that VZV-infected PDC culture supernatant did not induce significant levels of IFN-α secretion by uninfected PDC (Fig. 8). When treated with ODN2216, both uninfected PDC and uninfected PDC incubated with supernatant from infected PDC cultures secreted high levels of IFN-α, indicating that incubation of uninfected PDC with the cell supernatant from infected PDC cultures did not block their capacity to respond to ODN2216.

DISCUSSION

DC are potent antigen-presenting cells found throughout the body, particularly at sites of pathogen entry, such as mucosal and skin surfaces, where they play a critical role in antiviral immunity (33). However, little is known about the role of different DC subsets in the pathogenesis of VZV and other viruses. Assessment of naturally infected human tissues is challenging, and there is a paucity of studies examining DC in intact tissues during human infection with any virus. This study defines the type and distribution of changes in DC subsets which occur in the skin of individuals suffering from varicella or herpes zoster. We demonstrated a significant decrease in the frequency of LC concomitant with an influx of PDC in VZV-infected skin compared to findings for uninfected skin. We also observed sporadic VZV antigen-positive LC in the epidermis and VZV antigen-positive PDC within regions of cellular infiltrate in the dermis. The type of VZV antigen staining of these cells was consistent with replicating virus, suggesting that some of these DC become infected *in vivo*. We extended these analyses to demonstrate that both PDC and MUTZ-3-derived LC are permissive to VZV infection, but surprisingly, PDC do not respond to infection by secreting high

levels of IFN-α. This study defines the repertoire of changes in the response of DC and provides evidence for the infection of specific DC subtypes during natural cutaneous VZV infection.

The frequency of $CD1a^+$ $langerin^+$ LC was strikingly reduced in VZV-infected skin epidermis compared to that in uninfected skin, extending an earlier case report of CD1a expression in VZV-infected skin (51). This apparent reduction in the number of LC during VZV infection may be a consequence of (i) loss of expression of CD1a and langerin by LC which remain in the skin, (ii) cell death, or (iii) rapid migration of these cells out of the skin. In this study, we were able to show the presence of LC that stained positive for VZV antigens indicative of virus replication. On these cells, langerin staining remained abundant compared to nearby uninfected LC. In addition, staining of VZV-infected MUTZ-3-derived LC for langerin showed that the expression of this protein remained comparable to that in mock-infected cells (data not shown). Taken together, these data indicated that VZV infection of LC *in vivo* and MUTZ-3-derived LC *in vitro* did not adversely affect the expression of langerin. Terminal deoxynucleotidyltransferase-mediated dUTP-biotin nick end labeling (TUNEL) staining to detect damaged DNA of apoptotic cells performed on VZV-infected MUTZ-3-derived LC did not induce any significant level of apoptosis (data not shown). Taken together with our previous demonstration that MDDC do not undergo apoptosis following infection with VZV (1), it suggests that the reduced LC frequency in the epidermis was not due to apoptosis. Our results are therefore consistent with the reduction in LC numbers in VZV-infected skin being a consequence of LC emigration to distal sites, such as lymph nodes, where additional T-lymphocyte priming may occur. In the context of this hypothesis, the almost complete loss of LC from the skin suggests that bystander LC capture VZV antigen in the skin, stimulating LC emigration, and/or that LC carrying no viral antigen are stimulated to emigrate. In addition, our finding that LC are permissive to VZV replication *in vivo* raises the intriguing possibility that those LC which become infected with VZV (as opposed to those which capture viral antigen) may play a role in virus spread. These possible outcomes highlight the complexity of VZV-LC interactions in the skin. The establishment of a fresh human skin explant model of VZV infection, such as that described by Taylor and Moffat (57), could potentially be adapted to enable capture and characterization of any cells emigrating from the epidermis to further investigate the consequences of cutaneous VZV infection for LC function.

These findings implicate LC in VZV pathogenesis at the skin and also raise the prospect that LC present in the respiratory mucosa may be involved in the early stages of VZV pathogenesis. Mucosal membranes have been shown to contain LC that survey the mucosa for foreign antigens (27), and our hypothesis is that LC present in the respiratory mucosa are the first cells to become infected with VZV and travel to the lymph nodes, where they then infect T lymphocytes with VZV. VZV-infected T lymphocytes then migrate to the skin as part of the inflammatory infiltrate (40, 51, 58), where they are among the cells responsible for spreading VZV to cutaneous cells. The development of lesions in the typical course of varicella occurs in crops over several days (7), and our findings in the skin of infected patients support the notion that following the initial infiltration of VZV-infected immune cells, cutaneous LC become infected with VZV and emigrate to distal sites, such as draining lymph nodes, to infect additional T lymphocytes that then migrate to the skin to cause additional skin lesions.

Our characterization of the infiltrating cells in VZV skin lesions also revealed a prominent increase in the frequency of $CD123^+$ cells as determined by IHC and of $BDCA\text{-}2^+$ cells as determined by IFA in VZV infected-skin compared to findings for uninfected skin. CD123 and BDCA-2 are surface markers of PDC (15, 41), and although CD123 is also expressed by other cell types (41, 54, 59), BDCA-2 is exclusively expressed on PDC (15, 16). We observed similar frequencies and distribution of staining for these two markers in sections of VZV-infected skin lesions, which suggests that the majority of the $CD123^+$ cells identified by immunohistochemistry were PDC. We showed by dual immunofluorescent staining a small proportion of VZV $antigen^+$ PDC that stained positive for VZV antigens from all three VZV kinetic classes, indicating complete replication of VZV in PDC.

Despite only sporadic detection of VZV-infected PDC and LC during natural cutaneous infection, this finding is probably important when considered in the context of the frequency of infection of other cell types which were subsequently shown to play crucial roles in the course of natural VZV infection. For example, the proportion of VZV-infected lymphocytes in peripheral blood during natural VZV infection is very small, with estimates in the range of 1 in 100,000 PBMCs from healthy varicella patients becoming infected, yet the role of peripheral blood T cells in transporting virus to distal sites is regarded as a critical step in VZV pathogenesis (34, 35).

The skin biopsy specimens utilized for this study were obtained from different patients at different times after the appearance of either varicella or zoster rash. While it remains possible that changes to DC subtypes may be linked to the kinetics of the development of the lesion as virus replicates in the skin, we did not observe any significant temporal differences in the frequencies of DC subsets in the skin biopsy specimens that we examined. Correlation between timing of lesion formation and various DC subsets is complicated by the asynchronous appearance of lesions during varicella and zoster (2). That is, the age of an individual lesion within the rash may differ from the timing of the first appearance of the rash. A definitive answer to this question would require sequential biopsies of the same lesion area taken at multiple time points from the same donor starting from the initial appearance of the lesion, samples that would be difficult to obtain under ethical approval.

In a case study of a single varicella patient, a large number of infiltrating PDC were observed within the dermis of the varicella lesions, as determined by IHC staining for CD123 and BDCA-2, which coincided with reduced circulating PDC during the acute illness compared to levels after recovery (19). This implies that circulating PDC are recruited to the skin during varicella, presumably to contribute to the immune response against VZV. In this varicella case, large numbers of cells staining positive for MxA, an interferon-inducible protein and surrogate marker of IFN-α production, were observed in the epidermis and dermis, and since these cells were distributed in a manner similar to PDC distribution, it was concluded that the MxA^+ cells were PDC (19). However, these sections were not dually stained for BDCA-2 or CD123 and MxA, and

thus, it remains to be conclusively established whether the observed PDC are MxA^+. In addition, MxA is a protein that is induced by exogenous and endogenous IFN-α (1a, 52a, 60a), and although IFN-α-producing cells can respond to their own secreted IFN-α in an autocrine manner, MxA is also expressed by cells only responding to and not necessarily producing IFN-α (1a, 52a, 60a). Furthermore, this varicella case study did not determine whether VZV-infected PDC secreted IFN-α, since the presence of VZV antigen was not assessed. However, the observation of PDC in a varicella lesion does suggest some involvement of PDC in varicella. A more recent study has demonstrated $CD14^+$ monocytes within varicella lesions that express T-lymphocyte costimulatory molecules (20), and it was shown *in vitro* that monocytes can be induced by IFN-α to express T-lymphocyte costimulatory molecules and can then present VZV antigen to T lymphocytes (20). Given the previous observation of PDC and MxA^+ cells in varicella lesions (19), it was suggested that PDC in varicella lesions may secrete IFN-α that results in expression of T-lymphocyte costimulatory molecules by monocytes and subsequent presentation of VZV antigens to T lymphocytes (20). Our results show that PDC are recruited to the skin during cutaneous VZV infection, where a small number are infected. This influx of PDC was not accompanied by an increase in the number of cells expressing the mature DC marker (CD83), suggesting that PDC may not mature in VZV-infected skin. Our *in vitro* data support permissiveness of PDC to VZV and demonstrate that PDC do not respond to VZV infection by secreting significant amounts of IFN-α. Analysis of skin biopsy specimens from additional patients using dual-staining techniques will be an important goal of future studies to examine the maturation state of PDC and to determine the role of bystander and infected PDC in secretion of IFN-α during natural cutaneous infection. Furthermore, assessment of whether infiltrating PDC interact with T lymphocytes within VZV-infected skin will be important in establishing whether PDC may drive the immune response via interactions with T lymphocytes.

An influx of PDC has also been reported by us in recurrent genital herpes lesions caused by the closely related alphaherpesvirus herpes simplex virus type 2 (HSV-2) (14). PDC in genital herpes lesions were located in the dermis and at the dermo-epidermal junction in close proximity to T lymphocytes, particularly $CD69^+$ activated T lymphocytes. *In vitro* analysis found that despite expressing HSV glycoprotein D entry receptors, PDC do not become infected with HSV-2 and PDC exposed to HSV-2 were able to stimulate virus-specific autologous T-lymphocyte proliferation (14). Our finding that VZV could infect PDC *in vivo* and *in vitro* (with 40 to 70% of cells infected by 24 h postinfection) contrasts with findings for HSV-1 and HSV-2, which do not infect PDC (14, 44). In addition, while we found that VZV-infected PDC did not secrete significant amounts of IFN-α, we and others have reported that PDC exposed to HSV-1 or HSV-2 respond with abundant production of IFN-α (11, 14, 17). These findings point to fundamental differences between human alphaherpesviruses that replicate in the skin in the context of the permissiveness and response of PDC and indicate that VZV and HSV have evolved different strategies to cause disease in the human host.

PDC have also been shown to become infected with HIV, but these cells are still able to produce high levels of IFN-α (53–56). This suggests that general viral infection does not render PDC incapable of IFN-α production and that our observations of inhibited IFN-α production in VZV-inoculated PDC cultures may be due to a specific immune evasion mechanism encoded by VZV. In this respect, a study of IFN-α production in varicella skin lesions that used pSTAT as an IFN-α marker found that the VZV-infected cells did not express pSTAT but that adjacent uninfected cells did (38). Although this particular study focused on IFN-α production by epidermal cells, which occurs by a different mechanism than in PDC since TLR9 is not expressed in the epidermis (4), it suggests that VZV can inhibit the IFN-α response in VZV-infected cells. Our finding that VZV-infected PDC cultures, which contained both infected and uninfected cells, produced little IFN-α even when treated with ODN2216 suggests that the uninfected PDC in these cultures may be rendered resistant to the effects of ODN2216, perhaps as a consequence of a factor(s) secreted from VZV-infected PDC in the same culture. However, when supernatants were collected from infected PDC cultures and then added to uninfected PDC, these uninfected PDC retained the capacity to respond to ODN2216 and upregulate IFN-α. These observations raise the intriguing possibility that direct contact between VZV-infected and uninfected cells in the same culture may affect the capacity of uninfected PDC to express IFN-α in response to ODN2216. In this respect, we note two recent papers which report that PDC function was dependent on cell-to-cell contact in addition to secreted factors (10, 13). These reports did not look specifically at IFN-α, so examination of the control of this cytokine during VZV infection of PDC will be an important component of future work to define the nature of any direct functional interaction between VZV-infected PDC and uninfected bystander PDC. Likewise, it will be important to further define VZV-encoded modulation of IFN-α production by PDC to identify any viral gene which encodes this function. Together with the definition of changes which occur in the distribution of multiple DC subsets in the skin of individuals suffering from primary and recurrent VZV disease and the identification of LC and PDC as subsets most affected during infection, this study implicates the importance of VZV-mediated control of DC function in VZV pathogenesis.

ACKNOWLEDGMENTS

We thank Paul Kinchington from the University of Pittsburgh for VZV antigen-specific antibodies. We also thank Anthony Henwood of the Children's Hospital, Westmead, Australia, and Mark Wallace of the Infectious Diseases Division, Naval Medical Centre, San Diego, CA, for supplying skin samples, Rik Scheper of the Department of Pathology, VU University Medical Center, Amsterdam, Netherlands, for assistance with MUTZ-3-derived Langerhans cell culture, and Heather Donaghy of the Centre for Virus Research, Westmead Millennium Institute, for assistance with plasmacytoid dendritic cell culture.

This work was supported by Australian National Health and Medical Research Council Project Grant 457356. J.H.H. was the recipient of an Australian Postgraduate Award and a Westmead Millennium Institute Stipend Enhancement Award.

REFERENCES

1. **Abendroth, A., G. Morrow, A. L. Cunningham, and B. Slobedman.** 2001. Varicella-zoster virus infection of human dendritic cells and transmission to T cells: implications for virus dissemination in the host. J. Virol. **75:**6183–6192.

1a. **Aebi, M., J. Fäh, N. Hurt, C. E. Smuel, D. Thomis, L. Bazzigher, J. Pavlovic, O. Haller, and P. Staeheli.** 1989. cDNA structures and regulation of two interferon-induced human Mx proteins. Mol. Cell. Biol. **9:**5062–5072.

2. **Annunziato, P., O. Lungu, A. Gershon, D. N. Silvers, P. LaRussa, and S. J. Silverstein.** 1996. In situ hybridization detection of varicella zoster virus in paraffin-embedded skin biopsy samples. Clin. Diagn. Virol. **7:**69–76.

3. **Arvin, A. M., J. F. Moffat, and R. Redman.** 1996. Varicella-zoster virus: aspects of pathogenesis and host response to natural infection and varicella vaccine. Adv. Virus Res. **46:**263–309.

4. **Begon, E., L. Michel, B. Flageul, I. Beaudoin, F. Jean-Louis, H. Bachelez, L. Dubertret, and P. Musette.** 2007. Expression, subcellular localization and cytokinic modulation of Toll-like receptors (TLRs) in normal human keratinocytes: TLR2 up-regulation in psoriatic skin. Eur. J. Dermatol. **17:**497–506.

5. **Brunell, P. A.** 1967. Separation of infectious varicella-zoster virus from human embryonic lung fibroblasts. Virology **31:**732–734.

6. **Cella, M., D. Jarrossay, F. Facchetti, O. Alebardi, H. Nakajima, A. Lanzavecchia, and M. Colonna.** 1999. Plasmacytoid monocytes migrate to inflamed lymph nodes and produce large amounts of type I interferon. Nat. Med. **5:**919–923.

7. **Chen, T. M., S. George, C. A. Woodruff, and S. Hsu.** 2002. Clinical manifestations of varicella-zoster virus infection. Dermatol. Clin. **20:**267–282.

8. **Cohen, J. I., P. A. Brunell, S. E. Straus, and P. R. Krause.** 1999. Recent advances in varicella-zoster virus infection. Ann. Intern. Med. **130:**922–932.

9. **Colonna, M., G. Trinchieri, and Y. J. Liu.** 2004. Plasmacytoid dendritic cells in immunity. Nat. Immunol. **5:**1219–1226.

10. **Conry, S. J., K. A. Milkovich, N. L. Yonkers, B. Rodriguez, H. B. Bernstein, R. Asaad, F. P. Heinzel, M. Tary-Lehmann, M. M. Lederman, and D. D. Anthony.** 2009. Impaired plasmacytoid dendritic cell (PDC)-NK cell activity in viremic human immunodeficiency virus infection attributable to impairments in both PDC and NK cell function. J. Virol. **83:**11175–11187.

11. **Dai, J., N. J. Megjugorac, S. B. Amrute, and P. Fitzgerald-Bocarsly.** 2004. Regulation of IFN regulatory factor-7 and IFN-alpha production by enveloped virus and lipopolysaccharide in human plasmacytoid dendritic cells. J. Immunol. **173:**1535–1548.

12. **de Jong, M. A., L. de Witte, S. J. Santegoets, D. Fluitsma, M. E. Taylor, T. D. de Gruijl, and T. B. Geijtenbeek.** 30 December 2009. Mutz-3-derived Langerhans cells are a model to study HIV-1 transmission and potential inhibitors. J. Leukoc. Biol. [Epub ahead of print.]

13. **Ding, C., Y. Cai, J. Marroquin, S. T. Ildstad, and J. Yan.** 2009. Plasmacytoid dendritic cells regulate autoreactive B cell activation via soluble factors and in a cell-to-cell contact manner. J. Immunol. **183:**7140–7149.

14. **Donaghy, H., L. Bosnjak, A. N. Harman, V. Marsden, S. K. Tyring, T. C. Meng, and A. L. Cunningham.** 2009. A role for plasmacytoid dendritic cells in the immune control of human recurrent herpes simplex. J. Virol. **83:**1952–1961.

15. **Dzionek, A., A. Fuchs, P. Schmidt, S. Cremer, M. Zysk, S. Miltenyi, D. W. Buck, and J. Schmitz.** 2000. BDCA-2, BDCA-3, and BDCA-4: three markers for distinct subsets of dendritic cells in human peripheral blood. J. Immunol. **165:**6037–6046.

16. **Dzionek, A., Y. Sohma, J. Nagafune, M. Cella, M. Colonna, F. Facchetti, G. Gunther, I. Johnston, A. Lanzavecchia, T. Nagasaka, T. Okada, W. Vermi, G. Winkels, T. Yamamoto, M. Zysk, Y. Yamaguchi, and J. Schmitz.** 2001. BDCA-2, a novel plasmacytoid dendritic cell-specific type II C-type lectin, mediates antigen capture and is a potent inhibitor of interferon alpha/beta induction. J. Exp. Med. **194:**1823–1834.

17. **Feldman, S. B., M. Ferraro, H. M. Zheng, N. Patel, S. Gould-Fogerite, and P. Fitzgerald-Bocarsly.** 1994. Viral induction of low frequency interferon-alpha producing cells. Virology **204:**1–7.

18. **Fitzgerald-Bocarsly, P.** 1993. Human natural interferon-alpha producing cells. Pharmacol. Ther. **60:**39–62.

19. **Gerlini, G., G. Mariotti, B. Bianchi, and N. Pimpinelli.** 2006. Massive recruitment of type I interferon producing plasmacytoid dendritic cells in varicella skin lesions. J. Invest. Dermatol. **126:**507–509.

20. **Gerlini, G., G. Mariotti, A. Chiarugi, P. Di Gennaro, R. Caporale, A. Parenti, L. Cavone, A. Tun-Kyi, F. Prignano, R. Saccardi, L. Borgognoni, and N. Pimpinelli.** 2008. Induction of CD83+CD14+ nondendritic antigen-presenting cells by exposure of monocytes to IFN-alpha. J. Immunol. **181:**2999–3008.

21. **Gershon, A., L. Cosio, and P. A. Brunell.** 1973. Observations on the growth of varicella-zoster virus in human diploid cells. J. Gen. Virol. **18:**21–31.

22. **Gilden, D. H., A. Vafai, Y. Shtram, Y. Becker, M. Devlin, and M. Wellish.** 1983. Varicella-zoster virus DNA in human sensory ganglia. Nature **306:**478–480.

23. **Grose, C.** 1981. Variation on a theme by Fenner: the pathogenesis of chickenpox. Pediatrics **68:**735–737.

24. **Grose, C., and T. I. Ng.** 1992. Intracellular synthesis of varicella-zoster virus. J. Infect. Dis. **166:**S7–S12.

25. **Grose, C., D. M. Perrotta, P. A. Brunell, and G. C. Smith.** 1979. Cell-free varicella-zoster virus in cultured human melanoma cells. J. Gen. Virol. **43:**15–27.

26. **Heininger, U., and J. F. Seward.**2006. Varicella. Lancet **368:**1365–1376.

27. **Hellquist, H. B., K. E. Olsen, K. Irander, E. Karlsson, and L. M. Odkvist.** 1991. Langerhans cells and subsets of lymphocytes in the nasal mucosa. APMIS **99:**449–454.

28. **Hood, C., A. L. Cunningham, B. Slobedman, R. A. Boadle, and A. Abendroth.** 2003. Varicella-zoster virus-infected human sensory neurons are resistant to apoptosis, yet human foreskin fibroblasts are susceptible: evidence for a cell-type-specific apoptotic response. J. Virol. **77:**12852–12864.

29. **Hu, H., and J. I. Cohen.** 2005. Varicella-zoster virus open reading frame 47 (ORF47) protein is critical for virus replication in dendritic cells and for spread to other cells. Virology **337:**304–311.

30. **Iwasaki, T., R. Muraki, T. Kasahara, Y. Sato, T. Sata, and T. Kurata.** 2001. Pathway of viral spread in herpes zoster: detection of the protein encoded by open reading frame 63 of varicella-zoster virus in biopsy specimens. Arch. Virol. Suppl. **2001:**109–119.

31. **Kinchington, P. R., K. Fite, and S. E. Turse.** 2000. Nuclear accumulation of IE62, the varicella-zoster virus (VZV) major transcriptional regulatory protein, is inhibited by phosphorylation mediated by the VZV open reading frame 66 protein kinase. J. Virol. **74:**2265–2277.

32. **Kinchington, P. R., and J. I. Cohen.** 2000. Viral proteins, p. 74–104. *In* A. M. Arvin and A. A. Gershon (ed.), Varicella-zoster virus. Virology and clinical management. Cambridge University Press, Cambridge, United Kinggdom.

33. **Klagge, I. M., and S. Schneider-Schaulies.** 1999. Virus interactions with dendritic cells. J. Gen. Virol. **80:**823–833.

34. **Koropchak, C. M., G. Graham, J. Palmer, M. Winsberg, S. F. Ting, M. Wallace, C. G. Prober, and A. M. Arvin.** 1991. Investigation of varicella-zoster virus infection by polymerase chain reaction in the immunocompetent host with acute varicella. J. Infect. Dis. **163:**1016–1022.

35. **Koropchak, C. M., S. M. Solem, P. S. Diaz, and A. M. Arvin.** 1989. Investigation of varicella-zoster virus infection of lymphocytes by in situ hybridization. J. Virol. **63:**2392–2395.

36. **Krug, A., S. Rothenfusser, V. Hornung, B. Jahrsdorfer, S. Blackwell, Z. K. Ballas, S. Endres, A. M. Krieg, and G. Hartmann.** 2001. Identification of CpG oligonucleotide sequences with high induction of IFN-alpha/beta in plasmacytoid dendritic cells. Eur. J. Immunol. **31:**2154–2163.

37. **Ku, C. C., J. A. Padilla, C. Grose, E. C. Butcher, and A. M. Arvin.** 2002. Tropism of varicella-zoster virus for human tonsillar CD4(+) T lymphocytes that express activation, memory, and skin homing markers. J. Virol. **76:**11425–11433.

38. **Ku, C. C., L. Zerboni, H. Ito, B. S. Graham, M. Wallace, and A. M. Arvin.** 2004. Varicella-zoster virus transfer to skin by T Cells and modulation of viral replication by epidermal cell interferon-alpha. J. Exp. Med. **200:**917–925.

39. **Larsson, K., M. Lindstedt, and C. A. Borrebaeck.** 2006. Functional and transcriptional profiling of MUTZ-3, a myeloid cell line acting as a model for dendritic cells. Immunology **117:**156–166.

40. **Leinweber, B., H. Kerl, and L. Cerroni.** 2006. Histopathologic features of cutaneous herpes virus infections (herpes simplex, herpes varicella/zoster): a broad spectrum of presentations with common pseudolymphomatous aspects. Am. J. Surg. Pathol. **30:**50–58.

41. **Macardle, P. J., Z. Chen, C. Y. Shih, C. M. Huang, H. Weedon, Q. Sun, A. F. Lopez, and H. Zola.** 1996. Characterization of human leucocytes bearing the IL-3 receptor. Cell Immunol. **168:**59–68.

42. **Mahalingam, R., M. Wellish, W. Wolf, A. N. Dueland, R. Cohrs, A. Vafai, and D. Gilden.** 1990. Latent varicella-zoster viral DNA in human trigeminal and thoracic ganglia. N Engl. J Med. **323:**627–631.

43. **Masterson, A. J., C. C. Sombroek, T. D. De Gruijl, Y. M. Graus, H. J. van der Vliet, S. M. Lougheed, A. J. van den Eertwegh, H. M. Pinedo, and R. J. Scheper.** 2002. MUTZ-3, a human cell line model for the cytokine-induced differentiation of dendritic cells from CD34+ precursors. Blood **100:**701–703.

44. **Megjugorac, N. J., E. S. Jacobs, A. G. Izaguirre, T. C. George, G. Gupta, and P. Fitzgerald-Bocarsly.** 2007. Image-based study of interferongenic interactions between plasmacytoid dendritic cells and HSV-infected monocyte-derived dendritic cells. Immunol. Invest. **36:**739–761.

45. **Morrow, G., B. Slobedman, A. L. Cunningham, and A. Abendroth.** 2003. Varicella-zoster virus productively infects mature dendritic cells and alters their immune function. J. Virol. **77:**4950–4959.

46. **Muraki, R., T. Baba, T. Iwasaki, T. Sata, and T. Kurata.** 1992. Immunohistochemical study of skin lesions in herpes zoster. Virchows Arch. Pathol. Anat. Histopathol. **420:**71–76.

47. **Muraki, R., T. Iwasaki, T. Sata, Y. Sato, and T. Kurata.** 1996. Hair follicle involvement in herpes zoster: pathway of viral spread from ganglia to skin. Virchows Arch. **428:**275–280.

48. **Nikkels, A. F., S. Debrus, C. Sadzot-Delvaux, J. Piette, P. Delvenne, B. Rentier, and G. E. Pierard.** 1993. Comparative immunohistochemical study of herpes simplex and varicella-zoster infections. Virchows Arch. Pathol. Anat. Histopathol. **422:**121–126.

49. **Nikkels, A. F., S. Debrus, C. Sadzot-Delvaux, J. Piette, B. Rentier, and G. E. Pierard.** 1995. Localization of varicella-zoster virus nucleic acids and proteins in human skin. Neurology **45:**S47—S49.

50. **Nikkels, A. F., P. Delvenne, S. Debrus, C. Sadzot-Delvaux, J. Piette, B. Rentier, and G. E. Pierard.** 1995. Distribution of varicella-zoster virus gpI

and gpII and corresponding genome sequences in the skin. J. Med. Virol. **46:**91–96.

51. **Nikkels, A. F., C. Sadzot-Delvaux, and G. E. Pierard.** 2004. Absence of intercellular adhesion molecule 1 expression in varicella zoster virus-infected keratinocytes during herpes zoster: another immune evasion strategy? Am. J. Dermatopathol. **26:**27–32.
52. **Olding-Stenkvist, E., and M. Grandien.** 1976. Early diagnosis of virus-caused vesicular rashes by immunofluorescence on skin biopsies. I. Varicella, zoster and herpes simplex. Scand. J. Infect. Dis. **8:**27–35.

52a. **Roers, A., H. K. Hochkeppel, M. A. Horisberger, A. Hovanessian, and O. Haller.** 1994. MxA gene expression after live virus vaccination: a sensitive marker for endogenous type I interferon. **169:**807–813.

53. **Roizman, B., and J. Baines.** 1991. The diversity and unity of Herpesviridae. Comp. Immunol. Microbiol. Infect. Dis. **14:**63–79.
54. **Rothenberg, M. E., W. F. Owen, Jr., D. S. Silberstein, J. Woods, R. J. Soberman, K. F. Austen, and R. L. Stevens.** 1988. Human eosinophils have prolonged survival, enhanced functional properties, and become hypodense when exposed to human interleukin 3. J. Clin. Invest. **81:**1986–1992.
55. **Santegoets, S. J., A. J. van den Eertwegh, A. A. van de Loosdrecht, R. J. Scheper, and T. D. de Gruijl.** 2008. Human dendritic cell line models for DC differentiation and clinical DC vaccination studies. J. Leukoc. Biol. **84:**1364–1373.
56. **Siegal, F. P., N. Kadowaki, M. Shodell, P. A. Fitzgerald-Bocarsly, K. Shah, S. Ho, S. Antonenko, and Y. J. Liu.** 1999. The nature of the principal type 1 interferon-producing cells in human blood. Science **284:**1835–1837.
57. **Taylor, S. L., and J. F. Moffat.** 2005. Replication of varicella-zoster virus in human skin organ culture. J. Virol. **79:**11501–11506.
58. **Tsukahara, T., and Y. Horiuchi.** 1996. Immunohistochemical study of cellular events in lesional skin during common virus infections. J. Dermatol. **23:**22–32.
59. **Valent, P., G. Schmidt, J. Besemer, P. Mayer, G. Zenke, E. Liehl, W. Hinterberger, K. Lechner, D. Maurer, and P. Bettelheim.** 1989. Interleukin-3 is a differentiation factor for human basophils. Blood **73:**1763–1769.
60. **Valladeau, J., and S. Saeland.** 2005. Cutaneous dendritic cells. Semin. Immunol. **17:**273–283.

60a. **von Wussow, P., D. Jakschies, H. K. Hochkeppel, C. Fibich, L. Penner, H. Deicher.** 1990. The human intracellular Mx-homologous protein is specifically induced by type I interferons. Eur. J. Immunol. **20:**2015–2019.

61. **Weller, T. H.** 1953. Serial propagation in vitro of agents producing inclusion bodies derived from varicella and herpes zoster. Proc. Soc. Exp. Biol. Med. **83:**340–346.
62. **Weller, T. H., H. M. Witton, and E. J. Bell.** 1958. The etiologic agents of varicella and herpes zoster; isolation, propagation, and cultural characteristics in vitro. J. Exp. Med. **108:**843–868.
63. **Zhang, Z., and F. S. Wang.** 2005. Plasmacytoid dendritic cells act as the most competent cell type in linking antiviral innate and adaptive immune responses. Cell Mol. Immunol. **2:**411–417.